Interaction between Resonant Magnetic Perturbations and Sheared Flows

A. Monnier[1], G. Fuhr[1], P. Beyer[1], S. Benkadda[1]

[1] *International Institute for Fusion Science / PIIM, Aix-Marseille Univ. , Marseille, France*

In tokamaks, improved confinement regimes allow to obtain sufficient core plasma temperatures to produce self-sustained nuclear fusion reactions. These regimes are characterised by transport barriers, i.e. radially thin layers where turbulent transport of heat and matter is significantly reduced leading to a strong increase of the pressure gradient. At the plasma edge, the transport barrier is typically unstable and exhibits quasi-periodic relaxations associated with high energy fluxes that can eventually damage the tokamak wall. These barrier relaxations are an essential characteristics of the so-called Edge Localized Mode (ELMs) [1]. The control of these modes is a critical issue for the next generation of experimental reactor such as ITER. Studies on tokamaks such as DIII-D [2], JET [3] and TEXTOR [4] reveal a qualitative control of ELMs by imposing external Resonant Magnetic Perturbations (RMPs) at the plasma edge.

The control of transport barrier relaxations by RMPs is generally due to a reduction of pressure gradient by a radial energy flux [5]. This property is generally attributed to the appearence of field line stochasticity for large RMP amplitudes. However, it is not clear to which extend the externally induced perturbation actually penetrates into the plasma. Magnetohydrodynamical (MHD) modeling has shown an effective screening of RMPs by a rotating plasma [6]. This screening has also been observed in numerical simulations with an effective velocity at the plasma egde [7].

In previous works, control of barrier relaxations have been studied by three-dimensional edge turbulent simulations in presence of externally induced RMPs [8]. Here, an extension of the previous electrostatic model is used taking into account self-consistent electromagnetic fluctuations [9]. The aim is to study the penetration of externally induced RMPs into the plasma. This will allow in a next step to investigate the effect of turbulence on the RMPs penetration and to study their impact on transport barrier relaxations.

The model equations used for the plasma pressure p, the electrostatic potential ϕ an the electromagnetic flux ψ are :

$$\begin{aligned}
(\partial_t + \vec{\mathbf{u}}_E \cdot \nabla) W &= -\frac{1}{\alpha}\nabla_\parallel J - \mathbf{G}p + \nu \nabla_\perp^2 W + \mu \left(W_{00} - W_{imp}\right), &(1)\\
(\partial_t + \vec{\mathbf{u}}_E \cdot \nabla) p &= \delta_c \mathbf{G}\phi + \chi_\parallel \nabla_\parallel^2 p + \chi_\perp \nabla_\perp^2 p + S(x), &(2)\\
\partial_t \psi &= -\nabla_\parallel \phi + \frac{1}{\alpha}\left(J - J_{RMP}\right). &(3)
\end{aligned}$$

Equation (1) corresponds to the vorticity equation, $W=\nabla_\perp^2\phi$ is the vorticity of the $\mathbf{E}\times\mathbf{B}$ flow $\vec{\mathbf{u}}_E$, $J=\nabla_\perp^2\psi$ is the parallel current fluctuation, α is proportional to the plasma β, i.e. the ratio of kinetic to magnetic pressure. $\mathbf{G}$ is the magnetic curvature operator, ν is the viscosity coefficient, μ is the friction coefficient with the imposed vorticity $W_{imp}=\nabla_\perp^2\phi_{imp}$. W_{00} corresponds to the axisymmetric component of W. Eq. (2) describes the energy conservation, $\chi_\parallel$ and $\chi_\perp$ are respectively the collisional heat diffusivities parallel and perpendicular to the magnetic field lines, δ_c is a curvature parameter, and $S(x)$ is an energy source modeling the constant heat flux from the plasma core. Eq. (3) corresponds to the Ohm's Law, J_{RMP} is the external current (Fig. 2b, solid curve) generating RMPs. Simultations are performed with the EMEDGE3D code [10]. Following the standard convention $x,\ y,\ z$ represent respectively the normalized local radial, poloidal and toroidal coordinates. Introducing the safety factor $q(x)$, the main computational domain corresponds to the volume delimited by the toroidal surfaces $q_{min}=2.5$ and $q_{max}=3.5$ (Fig. 1a, vertical black dash lines). The energy source $S(x)$ (Fig. 1b, heat flux profile) is located in the region $q<q_{min}$.

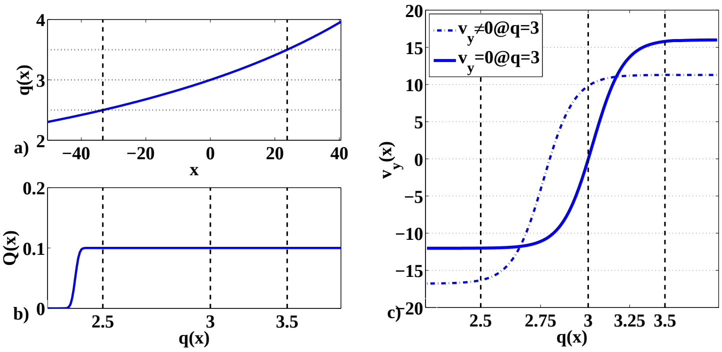

Figure 1: Radial profiles of safety factor q (a), heat flux $Q(x)=\int^x\frac{S(x')}{\chi_\perp}dx'$ (b) and poloidal velocity (c).

In this work, the RMPs penetration is studied with an imposed sheared $\mathbf{E}\times\mathbf{B}$ rotation in the poloidal direction. Looking for a stationary state of the form $(\phi,\ \psi)=(\phi_{00},0)+(\phi_{mn},\ \psi_{mn})\,(x)e^{i\left(m\kappa_y y-n\kappa_z z\right)}+c.c.$ corresponding to a single harmonic perturbation with mode numbers $m\kappa_y$ and $n\kappa_z$ in the y (poloidal) and z (toroidal) directions, respectively, the Ohm's law (Eq. (3)) becomes :

$$0=i\left(n-\frac{m}{q(x)}\right)\kappa_z\phi_{mn}-im\kappa_y\psi_{mn}\partial_x\phi_{00}+\frac{1}{\alpha}\nabla_\perp^2\psi_{mn} \qquad (4)$$

From this Eq. (4), with a plasma rotation ($\bar{v}_y=\partial_x\phi_{00}\neq0$) at the resonant surface $q={}^m/_n$, a current response is expected J_{mn} and so the screening of the RMP. Vice-versa, if penetration of the RMP appears, plasma rotation vanishes at the resonant surface. The efficiency of the screening as a function of rotation velocity and perturbation amplitude is studied now with the full electromagnetic turbulence model. In the cases considered here, the total heat flux and the corresponding pressure gradient are below the resistive ballooning instability limit.

For a single harmonic perturbation, the external current is chosen as $J_{RMP}^{single}=\nabla_\perp^2\psi_{RMP}^{single}$ with $\psi_{RMP}^{single}=\psi_0\psi_{m_0}(x)\cos\left(m_0\kappa_y y-n_0\kappa_z z\right)$, ψ_0 is the overall perturbation amplitude, $\psi_{m_0}(x)$ describes the radially increasing perturbation in the vaccum case [8]. The perturbation with wavenumbers $(m_0,n_0)=(12,4)$ is resonant at $q=q_0=3$. To quantify the screening of the perturbation by the

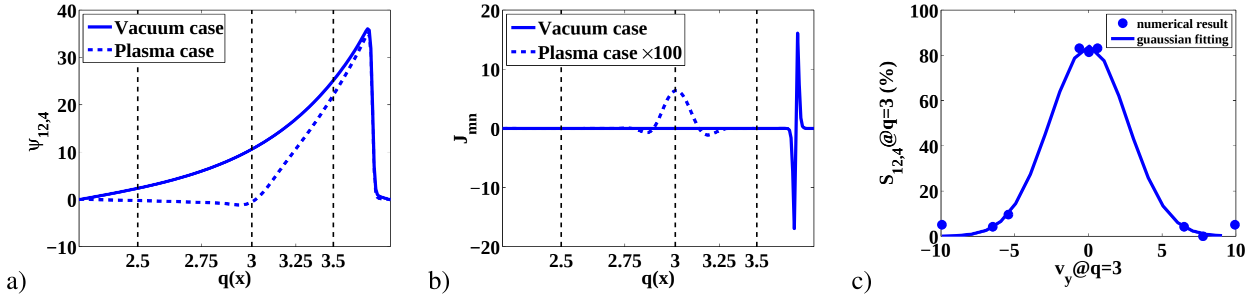

Figure 2: Radial profiles of $\psi_{m_0 n_0}$ (a), $J_{m_0 n_0}$ (b) in vacuum case (solid curve) and with plasma ($J_{m_0 n_0} \times 100$, dash), and screening factor (c) for different values of $\bar{v}_y\,(q=3)$.

plasma, a reference case artificially suppressing the plasma response, i.e. the parallel electric field $\nabla_{\parallel}\phi$ in the Ohm's law, is performed. The resulting radial profiles of ψ_{RMP}^{single} and J_{RMP}^{single} in this case are shown in Figs. 2a and Figs. 2b (solid curve), respectively.

This simulation is compared with a self-consistent case including the plasma response and an externally imposed poloidal rotation such that $\bar{v}_y \neq 0$ at the resonant surface $q = q_0$ (Fig. 1c, dash curve). With respect to the vacuum case, the magnetic perturbation is strongly reduced (Fig. 2a) by a screening current at the resonant surface (Fig. 2b). Screening can be quantified via the factor $S_{mn} = {|\psi_{mn}(q={m}/{n})|}/{|\psi_{mn}^{vac}(q={m}/{n})|}$ as a function of the velocity at $q_0 = {m_0}/{n_0}$. The velocity at the resonant surface is modified by displacing the velocity profile in the radial direction (Fig. 2c). When the plasma is at rest at the resonant surface, $\bar{v}_y(q={m}/{n}) \approx 0$, the RMP penetrates with $S_{m_0 n_0} \geq 80\%$. On the contrary, if the plasma rotates at the resonant surface, the screening factor is below 10%. Note that the velocity profiles considered here are known to generate transport barriers in this resistive balloning model [8, 10]. Moreover, the observed behavior of the screening factor qualitatively agrees with results from more sophisticated models [7].

In tokamak experiments, RMPs contain multiple harmonic [8]. To study the impact of multiplicity of present harmonics, a perturbation containing all poloidal resonant modes for one toroidal mode ($n_0 = 4$) is implemented :

$$J_{RMP}^{multiple} = \nabla_{\perp}^2 \psi_{RMP}^{multiple} \text{ with } \psi_{RMP}^{multiple} = \psi_0 \sum_{m=q_{min}n_0}^{m=q_{max}n_0} (-1)^m \,\psi_m(x) \cos\left(m\kappa_y y - n_0 \kappa_z z\right),$$

the poloidal spectrum of the perturbation is represented by $\psi_m(x)$ ([8] for details). In the case presented here with $\bar{v}_y(q_0 = 3) \approx 0$ (Fig. 1c, solid curve), only the mode $m_0 = q_0 n_0 = 12$ penetrates ($\psi_{m_0 n_0} \neq 0$), and all the other modes vanish on their corresponding resonant surfaces (Fig. 3a). This result is explained by the associated current (Fig. 3b). Except for the $m = 12$ mode, a current is generated at the positions corresponding to $q = 2.5$, 2.75, 3.25 and 3.5, i.e. the resonant surface for the $m = 10$, 11, 13 and 14 modes.

The impact of the overall perturbation amplitude ψ_0 on the screening factor is plotted on Fig. 3c.

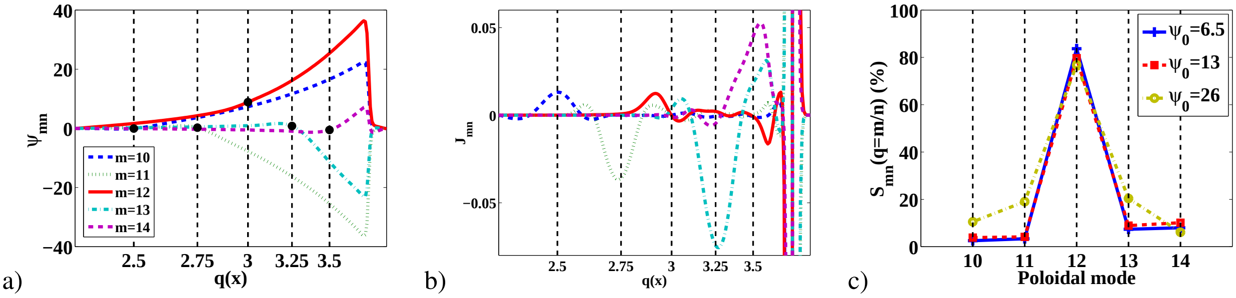

Figure 3: $\psi_{m,4}$ (a) and $J_{m,4}$ (b) for $m = 10 \rightarrow 14$. Screening factor (c) as a function of m and ψ_0. (a) Full circles correspond to $\psi_{m,4}(q = {}^{m}/_{4})$.

The $m = 12$ mode, which penetrates, is not affected by the modification of ψ_0 (screening value $S_{12,4} > 80\%$). At the opposite, for the other modes, the screening factor increases with increasing RMP amplitude (Fig. 4c). Since the resonant surface associated with $m = 14$ is located on the simulation boundary, the impact of ψ_0 on the screening cannot be interpreted.

In conclusion, we study the penetration of RMPs via numerical simulations in a reduced MHD model using the three-dimensional electromagnetic turbulence code EMEDGE3D. In agreement with previous works, the screening of the external RMP increases with the plasma rotation and penetration only occurs if the velocity vanishes on the corresponding resonant surface. Moreover, the screening efficiency decreases with increasing RMP amplitude. In future work, since the model used here is abled to reproduce transport barriers and their relaxation dynamics, the next step will be to characterize the impact of self-consistently RMPs on barrier relaxations.

This work has been supported by the French National Research Agency, project ANR-2010-BLAN-940-01.

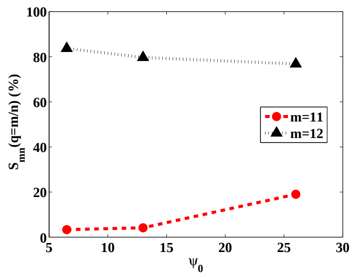

Figure 4: Screening factor as a function of perturbation amplitude for a screened mode ($m = 11$) and a penetrating mode ($m = 12$).

References

[1] Connor J.W. 1998 Plasma Phys. Control. Fusion **40** 531
[2] Evans T.E. *et al.* 2004 Phys. Rev. Lett. **92** 235003
[3] Liang Y. *et al.* 2007 Phys. Rev. Lett. **98** 265004
[4] Finken K.H. *et al.* 2007 Nucl. Fusion **47** 522
[5] Bécoulet M. *et al.* 2005 Nucl. Fusion **45** 1284
[6] Nardon E. *et al.* 2007 Phys. Plasmas **14** 092501
[7] Bécoulet M. *et al.* 2012 Nucl. Fusion **52** 054003
[8] Beyer P. *et al.* 2011 Plasma Phys. Control. Fusion **53** 054003
[9] Monnier A. *et al.* 2011 **38**th EPS Conf. on Controlled Fusion and Plasma Physics
[10] Fuhr G. *et al.* 2008 Phys. Rev. Lett. **101** 195001